

CogniEdit: Dense Gradient Flow Optimization for Fine-Grained Image Editing

Yan Li^{†§} Lin Liu[†] Xiaopeng Zhang[‡] Wei Xue[†]
 Wenhan Luo[†] Yike Guo[†] Qi Tian[‡]

[†] Hongkong University of Science and Technology [‡] Huawei Company

Abstract

Instruction-based image editing with diffusion models has achieved impressive results, yet existing methods struggle with fine-grained instructions specifying precise attributes such as colors, positions, and quantities. While recent approaches employ Group Relative Policy Optimization (GRPO) for alignment, they optimize only at individual sampling steps, providing sparse feedback that limits trajectory-level control. We propose a unified framework **CogniEdit**, combining multi-modal reasoning with dense reward optimization that propagates gradients across consecutive denoising steps, enabling trajectory-level gradient flow through the sampling process. Our method comprises three components: (1) Multi-modal Large Language Models for decomposing complex instructions into actionable directives, (2) Dynamic Token Focus Relocation that adaptively emphasizes fine-grained attributes, and (3) Dense GRPO-based optimization that propagates gradients across consecutive steps for trajectory-level supervision. Extensive experiments on benchmark datasets demonstrate that our CogniEdit achieves state-of-the-art performance in balancing fine-grained instruction following with visual quality and editability preservation.

1. Introduction

Instruction-based image editing enables users to manipulate images through natural language commands, offering an intuitive interface for visual content creation. Recent advances in diffusion models [26, 28] have achieved impressive results in generating high-quality edits that align with user instructions [5, 25, 35, 43]. However, critical limitations persist: existing methods [16, 39, 42] struggle with both fine-grained instruction following and reasoning-intensive editing tasks. They fail to accurately capture precise visual attributes such as exact colors, specific positions, or numerical quantities. Moreover, when faced with complex instructions requiring reasoning or domain knowl-

edge, these models exhibit an understanding gap between instruction semantics and editing demands [38], leading to edits that are semantically incorrect or factually implausible. These limitations stem from the training paradigm: most instruction-based editing models [5, 43] are trained through supervised learning on paired datasets, which primarily optimize for overall visual similarity between generated and target images. While this enables general editing capabilities, it does not explicitly optimize for fine-grained alignment between textual descriptions and specific visual attributes. As illustrated in Figure 1, existing methods struggle with numerical and spatial attributes, whereas our approach achieves superior alignment between instructions and visual attributes.

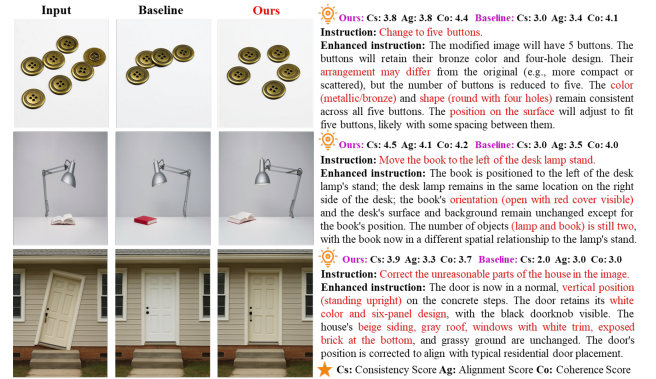


Figure 1. Comparison of editing results on instructions with fine-grained numerical and spatial attributes. We highlight three evaluation metrics: **Consistency** (visual consistency between edited and input images), **Coherence** (logical plausibility of edited content), and **Alignment** (instruction-image alignment), evaluated by Qwen2.5-VL-Think (7B) model.

Recently, reinforcement learning (RL) techniques have shown promise in aligning generative models with human preferences [4, 8, 9, 18, 30]. Group Relative Policy Optimization (GRPO) [29], in particular, has demonstrated success in text generation [20, 31] and image generation [23, 33, 40] by computing advantages relative to group statistics without requiring separate value networks. However, existing GRPO applications [23, 40] typically optimize each sampling step independently, treating each step

[§]For any inquiries, please reach out to: ylitiz@connect.ust.hk

as a separate decision point. This single-step optimization strategy fails to guide the overall sampling process while the model learns to improve individual steps, gradients do not flow through consecutive sampling steps, preventing dense supervision across the denoising process. For image editing, where consistency between source and edited regions is paramount [19, 32], this lack of gradient flow hinders fine-grained alignment and can lead to visual artifacts or convergence difficulties [37]. Achieving precise control over editing attributes while maintaining source consistency requires both fine-grained alignment between text features and visual content, and dense supervision across the sampling process to ensure edits evolve correctly from coarse structure to fine details.

To address these challenges, we propose a unified framework **CogniEdit**, combining multi-modal reasoning with dense reward optimization for instruction-based image editing. Our key insight is twofold: first, reasoning-intensive editing requires semantic understanding beyond visual pattern matching; second, fine-grained instruction following demands dense supervision throughout the editing process. We leverage Multi-modal Large Language Models (MLLMs) to decompose complex instructions into clear, actionable editing directives ensuring semantic correctness. For precise execution, we introduce two synergistic components: (i) *Dynamic Token Focus Relocation*, which adaptively emphasizes fine-grained attributes in reasoned instructions, and (ii) *Dense GRPO-based optimization*, which propagates gradients across consecutive denoising steps to enable gradient flow through the sampling trajectory. By unifying MLLM-based reasoning with trajectory-aware dense optimization, our method achieves both complex reasoning-intensive editing and precise fine-grained attribute control.

Our contributions can be summarized as follows:

- We address two critical limitations in existing image editing methods: understanding gap in reasoning-intensive tasks and sparse feedback in optimization by proposing a unified framework combining MLLM-based reasoning with dense reward optimization.
- We introduce a dynamic token focus relocation mechanism that enables adaptive attention to fine-grained attribute specifications in editing instructions, enhancing the model’s ability to capture precise visual details.
- We develop an efficient dense GRPO-based optimization mechanism with gradient propagates through sampling trajectory, achieving superior fine-grained instruction following while maintaining computational efficiency and training stability.

2. Related Work

2.1. General Image Editing

Instruction-based Image Editing. Instruction-based image editing enables users to manipulate images through natural language commands. Existing approaches can be categorized into training-free and training-based methods. Training-free methods [2, 6, 12, 13, 15, 19, 27, 45] manipulate attention mechanisms or incorporate guidance during diffusion, offering flexibility without model updates but often struggling with complex semantic edits. Training-based methods [3, 5, 16, 42, 43] learn from paired datasets of source images, instructions, and targets. InstructPix2Pix [5] pioneered this direction, while recent large-scale models such as Qwen-Image [35] and OmniGen [36, 39] achieve impressive general-purpose capabilities through massive pre-training. However, despite these advances, existing methods struggle with fine-grained instruction following, particularly when instructions require reasoning or domain knowledge. This limitation results in misalignment between textual instructions and visual content, motivating the integration of external knowledge and reasoning capabilities.

Knowledge-enhanced Image Editing. To handle instructions requiring reasoning or domain knowledge, recent methods leverage Multi-modal Large Language Models (MLLMs) to enhance semantic understanding [10, 21, 25, 32, 34, 41]. Step1X-Edit [25] and BrushEdit [21] employ MLLMs to jointly process images and instructions for reasoning about edit requirements. GenArtist [34] uses GPT-4 [1] as an agent to decompose complex tasks into simpler instructions. While these approaches improve semantic accuracy through better instruction understanding, they primarily focus on preprocessing instructions before generation. The generation process itself remains supervised learning on paired data, which does not explicitly optimize for fine-grained alignment between textual specifications and visual attributes.

In contrast, our method addresses fine-grained alignment through the optimization process itself. We combine MLLM-based reasoning with dynamic token focus relocation to enhance the model’s ability to capture fine-grained textual features from editing instructions, and dense reward optimization that provides supervision across consecutive sampling steps. This enables our method to achieve superior fine-grained instruction following and precise alignment between textual specifications and visual attributes.

2.2. Reinforcement Learning for Image Editing

Reinforcement learning has emerged as a powerful approach for aligning generative models with human preferences and complex objectives [4, 8, 9, 18, 30]. Group Relative Policy Optimization (GRPO) [29] offers an efficient RL framework that computes advantages relative

to group statistics without requiring separate value networks [23, 33, 40]. Recent work has begun adapting these techniques to image editing, focusing on improving instruction adherence and visual quality [17, 44]. However, existing approaches typically apply optimization at individual sampling steps, treating each step as an independent decision point. This sparse feedback strategy limits the model’s ability to learn trajectory-level guidance across the denoising process, hindering fine-grained control over specific editing attributes [9, 24, 37].

Our CogniEdit extends standard GRPO to dense reward optimization specifically designed for image editing. By accumulating gradients across consecutive sampling steps, we enable gradient flow through the denoising trajectory, providing dense supervision throughout the editing process. This trajectory-level optimization allows the model to learn fine-grained alignment between textual specifications and visual attributes while maintaining computational efficiency and training stability.

3. Methodology

Figure 2 presents an overview of our CogniEdit, which consists of three key components: (a) Dynamic Token Focus Relocation that adaptively emphasizes fine-grained attributes in instructions, (b) GRPO-based optimization adapted for image editing with batch-level advantage computation, and (c) Dense GRPO-based Optimization Supervision that propagates gradients across consecutive denoising steps to enable trajectory-level gradient flow.

3.1. GRPO for Image Editing

Group Relative Policy Optimization (GRPO) is a reinforcement learning technique designed to align generative models with human preferences through reward-based optimization. Unlike traditional policy gradient methods that require explicit value function estimation, GRPO operates by sampling multiple outputs from the current policy and using their relative rewards to compute policy gradients.

Standard Flow-Matching GRPO. For image generation with flow-matching models, GRPO adapts policy optimization to the continuous-time diffusion framework. Let v_θ denote the velocity network parameterized by θ , which predicts the direction of flow at each timestep. Given an input image and editing instruction c , GRPO samples a group of G generated images $\{x_0^1, x_0^2, \dots, x_0^G\}$ through the denoising process with T timesteps, where each sampling trajectory is determined by the policy π_θ induced by the velocity network. For each generated image x_0^i , we compute the reward $R(x_0^i, c)$ using a reward model. The advantage for the i -th sample is computed relative to the group statistics:

$$\hat{A}^i = \frac{R(x_0^i, c) - \frac{1}{G} \sum_{j=1}^G R(x_0^j, c)}{\text{std}(\{R(x_0^j, c)\}_{j=1}^G)} \quad (1)$$

where normalization by standard deviation stabilizes training. The policy is updated by maximizing the clipped objective, clip denotes the clip operation:

$$\mathcal{J}_{\text{GRPO}}(\theta) = \mathbb{E}_{\{c, x^i\}} \left[\frac{1}{G} \sum_{i=1}^G \frac{1}{T} \sum_{t=0}^{T-1} \min \left(r_i^t(\theta) \hat{A}^i, \text{clip}(r_i^t(\theta), 1 - \epsilon, 1 + \epsilon) \hat{A}^i \right) - \hat{\beta} D_{\text{KL}}(\pi_\theta \parallel \pi_{\text{ref}}) \right] \quad (2)$$

where $r_i^t(\theta) = \frac{p_\theta(x_{t-1}^i | x_t^i, c)}{p_{\theta_{\text{old}}}(x_{t-1}^i | x_t^i, c)}$ is the probability ratio at timestep t for the i -th sample, ϵ controls the clipping range to prevent large policy updates, and $\hat{\beta}$ balances the KL divergence term for regularization against a reference policy π_{ref} . The average over both group size G and timesteps T ensures stable gradient estimates. However, this formulation treats each timestep independently, limiting trajectory-level guidance.

Adapting GRPO for Image Editing. Image editing poses unique challenges compared to generation tasks. While generation tasks benefit from stochastic sampling to produce diverse outputs, editing tasks require high consistency and coherence with both the input image and editing instruction. Standard flow-matching models for editing use deterministic ODEs to ensure reproducible, consistent edits. However, this deterministic formulation presents a challenge for GRPO: sampling multiple outputs $\{x_0^i\}_{i=1}^G$ from a deterministic trajectory yields identical results, eliminating the diversity necessary for meaningful advantage computation.

To address this, we make two key adaptations. First, following [23], we inject controlled stochasticity into the sampling process by converting the deterministic ODE to an SDE via Euler-Maruyama discretization:

$$x_{t+\Delta t} = x_t + s_\theta(x_t, t) \Delta t + \sqrt{\Delta t} \sigma_t \epsilon \quad (3)$$

where $\epsilon \sim \mathcal{N}(0, 1)$, $s_\theta(x_t, t) = (v_\theta(x_t, t) + \sigma_t^2/2[x_t + (1-t)v_\theta(x_t, t)])$ and σ_t controls the noise level. This stochastic injection enables diverse sampling while maintaining editing quality through careful noise scheduling. Second, we compute advantages at the batch level rather than per-instance. Since editing outputs from the same input exhibit limited diversity even with stochastic sampling, per-instance advantage normalization produces high-variance gradients. By computing statistics across a batch of B editing instances, we obtain more stable advantage estimates: $\hat{A}^b = \frac{1}{G} \sum_{i=1}^G \frac{R(x_0^{b,i}, c_b) - \mu_{\text{batch}}}{\sigma_{\text{batch}}}$, where $\mu_{\text{batch}} = \frac{1}{BG} \sum_{b=1}^B \sum_{i=1}^G R(x_0^{b,i}, c_b)$, $\sigma_{\text{batch}} = \text{std}(\{R(x_0^{b,i}, c_b)\}_{b,i})$. The editing objective becomes:

$$\mathcal{J}_{\text{GRPO}}^{\text{edit}}(\theta) = \frac{1}{B} \sum_{b=1}^B \mathbb{E}_{\{c_b, x_0^b\}} \left[\frac{1}{T} \sum_{t=0}^{T-1} \min \left(r_b^t(\theta) \hat{A}^b, \text{clip}(r_b^t(\theta), 1 - \epsilon, 1 + \epsilon) \hat{A}^b \right) - \hat{\beta} D_{\text{KL}}(\pi_\theta \parallel \pi_{\text{ref}}) \right] \quad (4)$$

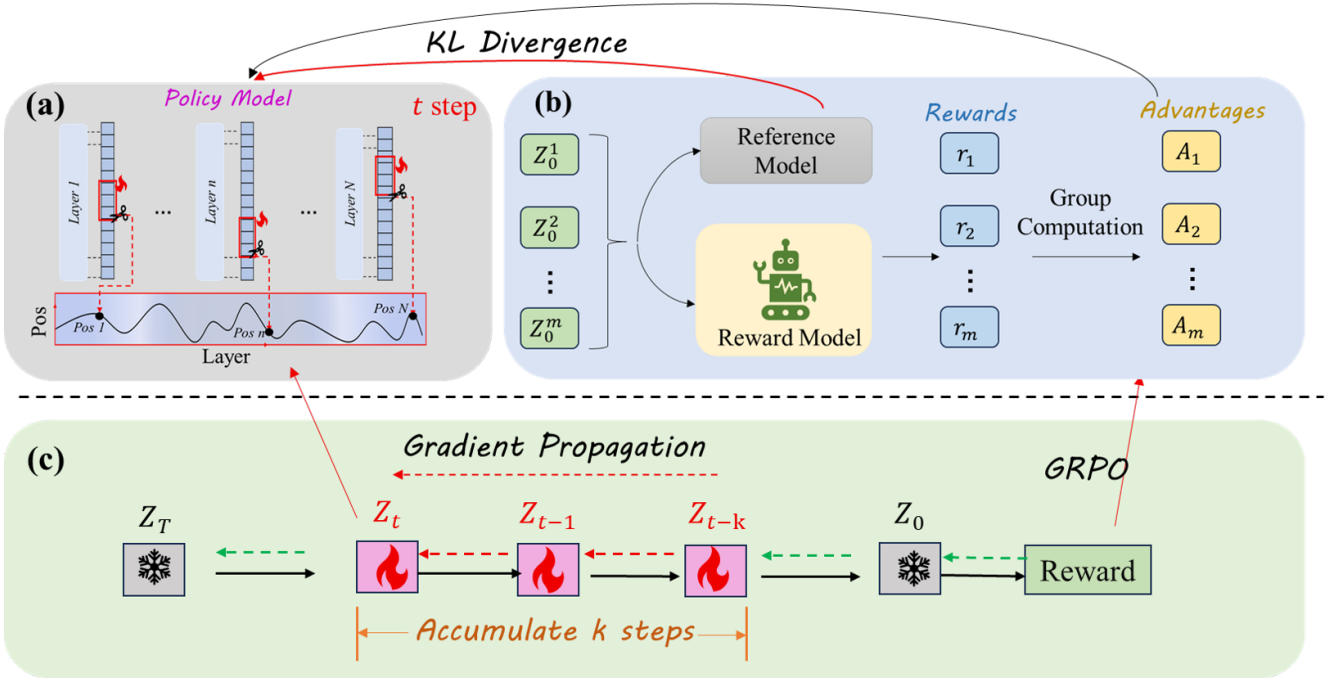


Figure 2. Overview of our proposed CogniEdit. (a) Dynamic token focus relocation mechanism for capturing fine-grained textual features. (b) Dense GRPO-based optimization strategy with gradient propagation at each sampling step. (c) Training process showing gradient accumulation over k consecutive steps.

where the superscript b indexes the batch and i indexes samples within each group. This batch-level normalization provides stable training dynamics while preserving the fine-grained control necessary for precise editing.

3.2. Dynamic Token Focus Relocation

A key challenge in instruction-based editing is ensuring the model attends to semantically relevant tokens at each processing stage. We observe that models often persistently attend to generic action words (e.g., “change”, “add”) throughout the network hierarchy while failing to process specific semantic details (e.g., “purple”, “five”, “on the left”) essential for accurate editing (as analyzed in Section 4.4.1). This issue becomes pronounced in complex instructions where different semantic components require emphasis at different stages—intuitively, early layers should focus on high-level semantics while deeper layers attend to fine-grained attributes. To address this, we propose Dynamic Token Focus Relocation that adaptively redirects attention to semantically important tokens in a layer-specific manner. Rather than relying on fixed attention patterns, our approach dynamically predicts which tokens are most relevant at different layers and uses learnable soft tokens to guide the model’s attention toward these positions, enabling different network layers to process different levels of semantic abstraction.

Formally, let $h_i^l \in \mathbb{R}^{l \times d}$ denote the encoded instruction

tokens at layer i , where l is the sequence length and d is the embedding dimension. We introduce a lightweight predictor p_η to identify the optimal attention focus position:

$$\text{pos} = p_\eta(h_i^l), \quad \text{pos} \in [0, l - \xi] \quad (5)$$

where k denotes the number of tokens to emphasize. The predictor is trained end-to-end to learn layer-specific attention patterns. Once the position is predicted, we enforce attention toward these positions using learnable soft tokens $s_i^{1:\xi} = E(i) \in \mathbb{R}^{\xi \times d}$ for each layer i , where E is a layer-dependent embedding function. These soft tokens serve as attention anchors and are injected into the instruction sequence at the predicted positions, replacing the original embeddings:

$$h_i^{\text{pos:pos}+\xi} \leftarrow s_i^{1:\xi}, \quad a_i^{\text{pos:pos}+\xi} = s_i^{1:\xi} \cdot A^l \quad (6)$$

where $A^l \in \mathbb{R}^{l \times l}$ is the attention map at layer l . The left equation replaces token embeddings, while the right equation computes attention scores using the injected soft tokens. Through joint optimization of the position predictor p_η and soft tokens $\{s_i^{1:\xi}\}_{i=1}^N$ across all N layers, the mechanism learns to dynamically emphasize different instruction components at appropriate depths. This results in hierarchical attention patterns where early layers focus on high-level semantics while deeper layers concentrate on fine-grained attributes, thereby improving instruction-image alignment.

3.3. Dense GRPO-based Optimization Supervision

In section 3.1, we introduce the how to adopt the GRPO-based optimization strategy for the image editing tasks. However, the standard GRPO-based optimization strategy optimized at single sampling step, and provide sparse feedback to the generation process. In diffusion-based image editing, each denoising step progressively refines the image, and the quality of these intermediate steps impacts the final result. A model that makes poor sampling decisions early in the generation process may struggle to recover in later steps, even with correct final-step optimization.

We propose Dense GRPO-based Optimization Supervision, which extends the standard GRPO objective to provide supervision at multiple intermediate sampling steps rather than only optimized at single sampling step. And to make the gradient propagation across the sampling trajectory, we adopt the stop gradient [37] operation to ensure the gradient flow back to the previous sampling step (we present the basic introduction in Appendix 7). The key insight is that by evaluating and optimizing the model’s decisions throughout the sampling trajectory, we can learn more nuanced control over the editing process and achieve better alignment.

To cover both early and later sampling steps, we randomly select a starting timestep $r \in [0, T-k]$ and perform k consecutive denoising steps, enabling gradient flow through the sampling trajectory. For each denoising step from t to $t-1$, the stochastic sampling process is:

$$x_{t-1} = x_t - 1/T s_\theta(sg(x_t), t) + \sigma_t/\sqrt{T}\epsilon \quad (7)$$

where $\epsilon \sim \mathcal{N}(0, I)$ is standard Gaussian noise, $v_\theta(x_t, t)$ is the predicted velocity at timestep t , and σ_t controls the noise injection level, $sg(\cdot)$ denotes the stop gradient operation. Starting from x_r at timestep r , we sequentially apply k denoising steps to obtain x_{r-k} , each intermediate state depends on the previous one, allowing gradients to flow backward through the entire k -step trajectory. Calculate the log of the probability ratios across the k -step trajectory:

$$\psi_b^{r:r-k}(\theta) = \sum_{t=r}^{r-k+1} \log \frac{p_\theta(x_{t-1}^b | x_t^b, c_b)}{p_{\theta_{\text{old}}}(x_{t-1}^b | x_t^b, c_b)} \quad (8)$$

then the $\tilde{r}_b^{r:r-k}(\theta) = \exp(\text{clip}(\psi_b^{r:r-k}(\theta), -\log(1+\epsilon), \log(1+\epsilon)))$. The Dense GRPO-based optimization objective for image editing becomes:

$$\mathcal{J}_{\text{Dense}}(\theta) = \mathbb{E}_{\tilde{r}, \{x_r^b, i\}} \left[\frac{1}{B} \sum_{b=1}^B \min \left(\tilde{r}_b^{r:r-k}(\theta) \hat{A}^b, \right. \right. \quad (9)$$

$$\left. \left. \text{clip}(\tilde{r}_b^{r:r-k}(\theta), 1-\epsilon, 1+\epsilon) \hat{A}^b \right) - \hat{\beta} D_{\text{KL}}(\pi_\theta \parallel \pi_{\text{ref}}) \right]$$

where \hat{A}^b is computed using the final reward after completing the denoising from x_{r-k} . This formulation enables gradient accumulation through consecutive sampling steps,

providing trajectory-level supervision rather than independent step-wise updates. By optimizing across the full sampling trajectory rather than just the endpoint, Dense Optimization Supervision provides denser supervision signals that guide the model to make better decisions at each stage of the generation process, leading to more stable training and improved editing quality.

4. Experiment

We conduct comprehensive experiments to validate our CognitionEdit’s effectiveness. Section 4.1 introduces the experiment settings, Section 4.2 presents quantitative and qualitative comparisons, Section 4.3 provides ablation studies and Section 4.4 analyzes key components.

4.1. Experimental Setup

4.1.1. Training Data Construction

Data Sources. We construct our training dataset by combining existing editing datasets with self-constructed data, resulting in a diverse collection of image editing pairs. Specifically, we utilize the following data sources:

- **SEED-Data-Edit [11]**¹: We sample 3k editing pairs from Part 2 of this dataset, which comprises real-world editing scenarios collected from the internet.
- **COCO 2017 [22]**²: We randomly select 1k images from the COCO 2017 dataset and construct corresponding editing pairs.

The details of data preparation process are presented in Appendix 8.2.

Knowledge-Enhanced Data Construction. To improve the quality and informativeness of editing instructions, we leverage a vision-language model (VLM) [7] to enrich the training data. Specifically, we feed both the source image and its corresponding editing instruction into the VLM, which generates a knowledge-enhanced instruction that incorporates additional semantic and contextual information about the scene. This enhanced instruction replaces the original one in the training data, providing more detailed guidance for the editing model. Figure 3 illustrates our knowledge-enhanced data construction pipeline. The construction details and samples are presented in Appendix 9.

4.1.2. Evaluation Protocol.

We conduct a comprehensive evaluation from two complementary perspectives: benchmark evaluation and human assessment. The details of human assessment can be found in Appendix 10.4.

Benchmark Evaluation. We evaluate our CognitionEdit on two complementary benchmarks that assess different as-

¹<https://huggingface.co/datasets/AILab-CVC/SEED-Data-Edit>

²<https://cocodataset.org/>

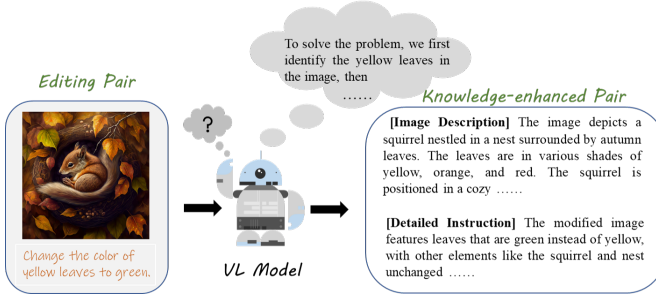


Figure 3. Illustration of the knowledge-enhanced data construction pipeline.

pects of image editing capabilities. KRIS-Bench [38], a diagnostic benchmark designed from a cognitively informed perspective, categorizes editing tasks into three foundational knowledge types based on educational theory: factual knowledge for fact-based edits, conceptual knowledge for abstract reasoning, and procedural knowledge for multi-step operations. The benchmark utilizes GPT-4-based assessment to measure performance across these cognitive dimensions. Additionally, we evaluate on GEdit-Bench [25], which collects authentic editing instances from real-world user scenarios to assess how well models handle genuine practical editing instructions and generalize to diverse editing challenges. We further conduct user study to evaluate the perceptual quality and editing fidelity of our CogniEdit compared to baseline approaches in Appendix 10.4.

4.1.3. Experiment Settings.

Implementation. We adopt Qwen-Image-Edit [35] as our base model, which provides strong vision-language understanding capabilities for image editing tasks. To enable efficient training while maintaining model performance, we employ parameter-efficient fine-tuning (PEFT) with Low-Rank Adaptation (LoRA) [14]. The LoRA rank is set to 4, which strikes an effective balance between model capacity and computational efficiency. We train our model for 500 steps using the AdamW optimizer with a learning rate of $1e-5$ and a batch size of 4. A linear warmup schedule is employed for the first 10% of training steps, followed by cosine learning rate decay. To prevent overfitting, we apply gradient clipping with a maximum norm of 1.0. The hyperparameter k is set to 5 and ξ is set to 64. All experiments are conducted on 8 NVIDIA A800 GPUs with 80GB memory each, more details of the implementations can be found in Appendix 10.

Baseline Methods. We compare our method against several state-of-the-art image editing approaches to demonstrate its effectiveness, including InstructPix2Pix [5], MagicBrush [43], AnyEdit [42], Step1X-Edit [25], OmniGen2 [36], Qwen-Image-Edit [35]. Additionally, to better assess the effectiveness of our method, we equip the Qwen-

Image-Edit with the VLM model to reason about the editing instructions as well. We denote this method as Qwen-Image-Edit-r1. We compare against these baselines using their official implementations and pretrained checkpoints to ensure fair evaluation.

4.2. Main Results

4.2.1. Quantitative Comparison.

Table 1 presents quantitative results on Kris-Bench, four metrics: VC (visual consistency), VQ (visual quality), IF (instruction following), and KP (knowledge preservation) averaged over all three domains (social science, natural science, and knowledge reasoning), evaluated by GPT-4.. Our CogniEdit achieves the highest visual quality scores across all three domains (social science, natural science, and knowledge reasoning), demonstrating superior perceptual quality while maintaining competitive performance in other metrics. In social science scenarios, we rank among the top-performing approaches, trailing only Qwen-Image-Edit-r1 in overall score while maintaining the lead in visual quality, and show strong performance across natural science and knowledge reasoning domains, validating effectiveness on diverse editing tasks requiring domain knowledge and reasoning capabilities. These results demonstrate that our dense optimization strategy effectively balances visual quality with instruction following, addressing the fundamental challenge of generating perceptually superior edits while maintaining semantic accuracy and content fidelity. The results of GEdit-Bench can be found in Appendix 10.2.

4.2.2. Qualitative Comparison.

Figure 4 presents qualitative comparisons with baseline methods. On Kris-Bench (Figure 4(a)), our CogniEdit demonstrates superior fine-grained instruction following: when instructions specify precise colors, positions, or quantities, our method accurately captures these details while maintaining high visual quality. In contrast, baseline methods often miss specific attributes or produce visually inconsistent results. This confirms that our dense reward optimization effectively guides the model toward both semantic accuracy and perceptual quality. On GEdit-Bench (Figure 4(b)), our CogniEdit preserves general editing capabilities across diverse scenarios from object removal to style transfer, with edited regions blending naturally with unchanged areas. This demonstrates that our specialized optimization for fine-grained alignment does not compromise general editing proficiency.

4.3. Ablation Study

To systematically validate the contribution of each component in our CogniEdit, we conduct comprehensive ablation studies on the Knowledge Reasoning category of the KRIS

Table 1. Results on Kris-Bench, where VC is the visual consistency score, VQ is the visual quality score, IF is the instruction following score, KP is the knowledge preservation score, and Avg is the average score.

Method	Social Science Science					Natural Science					Knowledge Reasoning				
	VC	VQ	IF	KP	Avg	VC	VQ	IF	KP	Avg	VC	VQ	IF	KP	Avg
InsPix2Pix	15.75	50.00	14.25	10.25	22.56	18.75	58.25	17.50	11.75	26.56	31.00	84.00	5.50	3.50	31.00
MagicBrush	54.00	70.00	27.25	20.50	42.94	47.00	72.25	19.00	13.50	38.06	62.50	88.75	11.25	8.25	42.69
AnyEdit	62.00	66.75	15.00	10.50	38.36	61.75	77.75	18.25	14.00	42.94	68.25	84.50	12.00	11.00	43.94
Step1X-Edit	78.50	77.75	28.75	22.75	51.94	82.75	79.00	28.00	21.00	52.69	78.75	81.25	20.00	14.00	48.50
OmniGen2	75.40	87.60	20.45	16.32	50.46	65.59	88.11	22.34	14.03	47.76	39.67	78.90	11.90	5.17	33.90
Qwen-Image-Edit	72.20	86.00	55.94	50.82	66.40	67.05	83.52	44.08	33.72	57.30	74.00	85.67	29.66	22.41	53.39
Qwen-Image-Edit-r1	79.20	89.14	73.17	70.53	77.99	72.07	87.60	52.88	46.40	64.78	71.33	88.37	35.03	27.55	55.48
CogniEdit	80.60	92.40	70.25	66.74	77.64	70.36	90.47	57.59	50.92	67.42	71.50	91.72	40.14	33.33	59.29

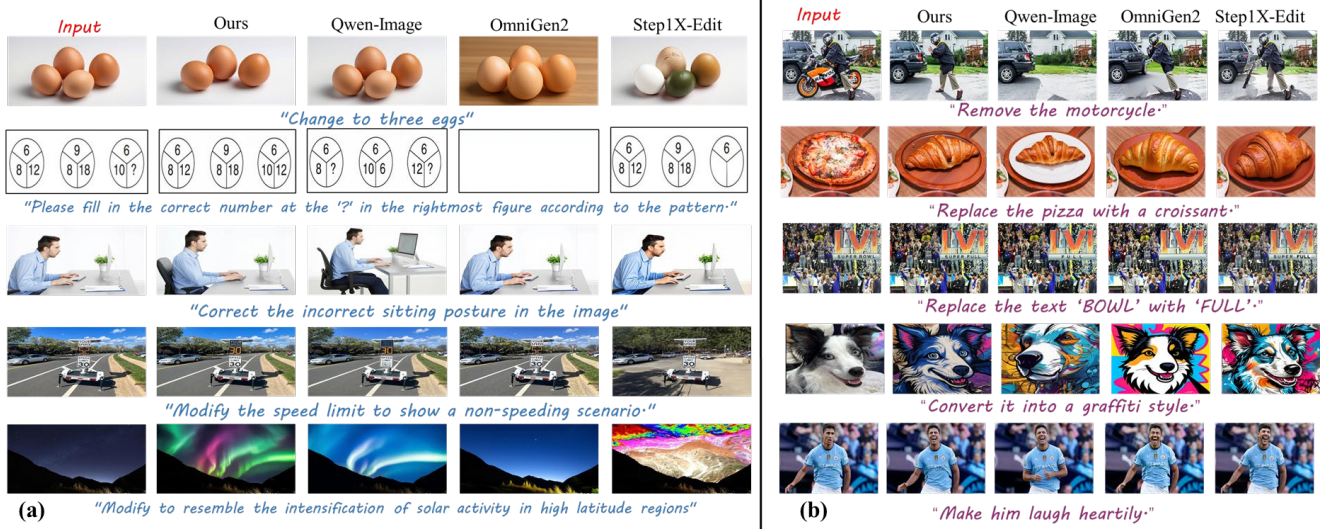


Figure 4. Qualitative comparison on Kris-Bench (a) and GEdit-Bench (b). Our CogniEdit achieves superior fine-grained instruction following while maintaining high visual quality and natural blending of edited regions.

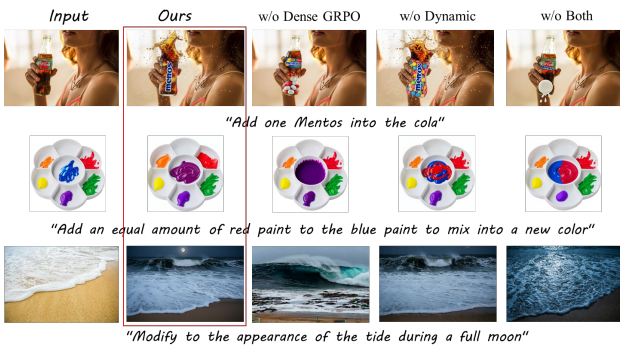


Figure 5. The visualization results of the ablation study.

benchmark. We evaluate three configurations: (1) removing Dense GRPO-based optimization while retaining Dynamic Text Alignment, (2) removing Dynamic token focus relocation while retaining Dense GRPO-based optimization, and

(3) removing both components, which effectively reverts to the base Qwen-Image-Edit-r1 model performance. This experimental design allows us to isolate the individual and synergistic effects of our proposed mechanisms.

Table 2. Ablation study results on the Knowledge Reasoning category. Each row shows performance when specific components are removed, demonstrating their individual contributions.

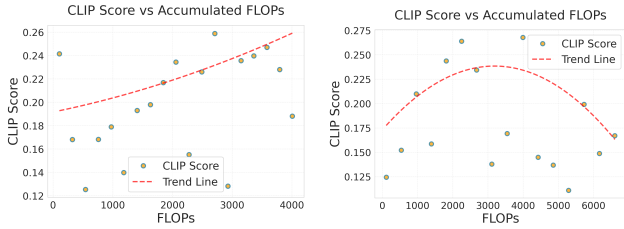
Method	Knowledge Reasoning				
	VC	VQ	IF	KP	Avg
w/o Dense GRPO	41.67	75.00	35.04	32.72	46.11
w/o Dynamic	62.67	86.17	41.73	36.09	54.66
w/o both (Base Model)	71.33	88.37	35.03	27.55	55.48
CogniEdit (Full Model)	71.50	91.72	40.14	33.33	59.29

Table 2 demonstrates that both components contribute substantially to our proposed CogniEdit’s performance. Removing Dense GRPO-based optimization causes the

most significant degradation, confirming its critical role in learning fine-grained semantic correspondences through trajectory-level supervision. Removing Dynamic Token Focus Relocation leads to moderate performance reduction, demonstrating its importance for hierarchical semantic understanding. The full model achieves 59.29, representing a notable improvement over the base model, which validates the synergistic effect of both mechanisms. Notably, the base model (w/o both) outperforms “w/o Dynamic” alone, indicating that Dynamic Token Focus Relocation is most effective when combined with Dense GRPO’s trajectory-level optimization, this complementary relationship highlights the importance of jointly optimizing attention patterns and reward signals for fine-grained editing.

4.4. Analysis of Key Components

4.4.1. Dense GRPO-based optimization.



(a) The CLIP score vs. FLOPs when with Dense GRPO. (b) The CLIP score vs. FLOPs when with standard GRPO.

To demonstrate the effectiveness of Dense GRPO, we analyze computational efficiency and optimization performance compared to standard GRPO. As shown in Figures 6a and 6b, Dense GRPO achieves superior performance with reduced computational overhead, exhibiting a steeper learning curve and greater training stability. This improvement stems from dense gradient flow through intermediate sampling steps, which provides more informative supervision signals throughout the generation trajectory. In contrast, standard GRPO shows erratic CLIP score fluctuations and limited capacity for fine-grained semantic correspondences due to sparse gradient signals computed only at sampling endpoints. By propagating gradients through the entire sampling process, Dense GRPO enables more effective optimization dynamics and better instruction-image alignment.

4.4.2. Dynamic Text Alignment Mechanism.

To analyze the effectiveness of Dynamic Token Focus Relocation, we conduct layer-wise analysis of attention patterns. Figure 7 compares attention distributions with (a) and without (b) our mechanism. With dynamic relocation, the model exhibits hierarchical attention allocation: for the instruction “Change the color of the purple eyes to red,” early layers prioritize abstract concepts (“the color”), intermediate layers shift to specific attributes (“purple,” “red”), and deeper

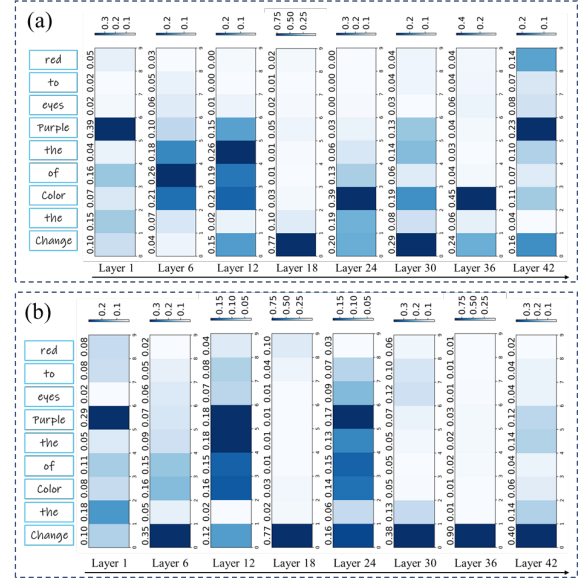


Figure 7. The attention maps from intermediate layers and the corresponding text importance scores with our proposed dynamic text alignment mechanism.

layers concentrate on actions (“change”). This hierarchical progression enables compositional understanding and precise semantic grounding. In contrast, without dynamic relocation, attention persistently focuses on “change” throughout all layers, resulting in incomplete semantic parsing and limited editing capabilities. These results demonstrate that dynamic attention reweighting across network depth effectively prioritizes semantically salient tokens at appropriate stages, yielding more accurate instruction-faithful editing.

5. Conclusion

We present a unified framework CogniEdit, for fine-grained instruction-based image editing that addresses two fundamental limitations: semantic understanding of complex instructions and sparse optimization feedback. Our approach combines multi-modal reasoning with dense reward optimization through three key components. First, we leverage Multi-modal Large Language Models to decompose complex instructions into semantically correct editing directives. Second, we introduce Dynamic Token Focus Relocation to enable hierarchical attention to fine-grained attributes across network layers. Third, we develop Dense GRPO-based optimization that propagates gradients across consecutive denoising steps, enabling trajectory-level supervision through the sampling process. Extensive experiments on Kris-Bench and GEdit-Bench demonstrate that our method achieves state-of-the-art performance in fine-grained instruction following while preserving general editing capabilities. These results validate that dense supervision across the sampling trajectory effectively balances precise attribute control with visual quality, providing a principled approach for instruction-based image editing.

References

- [1] Josh Achiam, Steven Adler, Sandhini Agarwal, Lama Ahmad, Ilge Akkaya, Florencia Leoni Aleman, Diogo Almeida, Janko Altschmidt, Sam Altman, Shyamal Anadkat, et al. Gpt-4 technical report. *arXiv preprint arXiv:2303.08774*, 2023. 2
- [2] Omri Avrahami, Or Patashnik, Ohad Fried, Egor Nemchinov, Kfir Aberman, Dani Lischinski, and Daniel Cohen-Or. Stable flow: Vital layers for training-free image editing. In *Proceedings of the Computer Vision and Pattern Recognition Conference*, pages 7877–7888, 2025. 2
- [3] Stephen Batifol, Andreas Blattmann, Frederic Boesel, Saksham Consul, Cyril Diagne, Tim Dockhorn, Jack English, Zion English, Patrick Esser, Sumith Kulal, et al. Flux. 1 kontext: Flow matching for in-context image generation and editing in latent space. *arXiv e-prints*, pages arXiv–2506, 2025. 2
- [4] Kevin Black, Michael Janner, Yilun Du, Ilya Kostrikov, and Sergey Levine. Training diffusion models with reinforcement learning. *arXiv preprint arXiv:2305.13301*, 2023. 1, 2
- [5] Tim Brooks, Aleksander Holynski, and Alexei A Efros. Instructpix2pix: Learning to follow image editing instructions. In *Proceedings of the IEEE/CVF conference on computer vision and pattern recognition*, pages 18392–18402, 2023. 1, 2, 6
- [6] Mingdeng Cao, Xintao Wang, Zhongang Qi, Ying Shan, Xiaohu Qie, and Yinqiang Zheng. Masactrl: Tuning-free mutual self-attention control for consistent image synthesis and editing. In *Proceedings of the IEEE/CVF international conference on computer vision*, pages 22560–22570, 2023. 2
- [7] Yan Chen, Long Li, Teng Xi, Long Zeng, and Jingdong Wang. Perception before reasoning: Two-stage reinforcement learning for visual reasoning in vision-language models. *arXiv preprint arXiv:2509.13031*, 2025. 5
- [8] Kevin Clark, Paul Vicol, Kevin Swersky, and David J Fleet. Directly fine-tuning diffusion models on differentiable rewards. *arXiv preprint arXiv:2309.17400*, 2023. 1, 2
- [9] Ying Fan, Olivia Watkins, Yuqing Du, Hao Liu, Moonkyung Ryu, Craig Boutilier, Pieter Abbeel, Mohammad Ghavamzadeh, Kangwook Lee, and Kimin Lee. Reinforcement learning for fine-tuning text-to-image diffusion models. In *Thirty-seventh Conference on Neural Information Processing Systems (NeurIPS) 2023*. Neural Information Processing Systems Foundation, 2023. 1, 2, 3
- [10] Tsu-Jui Fu, Wenze Hu, Xianzhi Du, William Yang Wang, Yinfei Yang, and Zhe Gan. Guiding instruction-based image editing via multimodal large language models. *arXiv preprint arXiv:2309.17102*, 2023. 2
- [11] Yuying Ge, Sijie Zhao, Chen Li, Yixiao Ge, and Ying Shan. Seed-data-edit technical report: A hybrid dataset for instructional image editing. *arXiv preprint arXiv:2405.04007*, 2024. 5, 4
- [12] Ligong Han, Song Wen, Qi Chen, Zhixing Zhang, Kunpeng Song, Mengwei Ren, Ruijiang Gao, Anastasis Stathopoulos, Xiaoxiao He, Yuxiao Chen, et al. Proxedit: Improving tuning-free real image editing with proximal guidance. In *Proceedings of the IEEE/CVF Winter Conference on Applications of Computer Vision*, pages 4291–4301, 2024. 2
- [13] Amir Hertz, Ron Mokady, Jay Tenenbaum, Kfir Aberman, Yael Pritch, and Daniel Cohen-Or. Prompt-to-prompt image editing with cross attention control.(2022). URL <https://arxiv.org/abs/2208.01626>, 3, 2022. 2
- [14] Edward J Hu, Yelong Shen, Phillip Wallis, Zeyuan Allen-Zhu, Yuanzhi Li, Shean Wang, Lu Wang, Weizhu Chen, et al. Lora: Low-rank adaptation of large language models. *ICLR*, 1(2):3, 2022. 6
- [15] Nisha Huang, Fan Tang, Weiming Dong, Tong-Yee Lee, and Changsheng Xu. Region-aware diffusion for zero-shot text-driven image editing. *arXiv preprint arXiv:2302.11797*, 2023. 2
- [16] Yuzhou Huang, Liangbin Xie, Xintao Wang, Ziyang Yuan, Xiaodong Cun, Yixiao Ge, Jiantao Zhou, Chao Dong, Rui Huang, Ruimao Zhang, et al. Smartedit: Exploring complex instruction-based image editing with multimodal large language models. In *Proceedings of the IEEE/CVF Conference on Computer Vision and Pattern Recognition*, pages 8362–8371, 2024. 1, 2
- [17] Nupur Kumari, Sheng-Yu Wang, Nanxuan Zhao, Yotam Nitzan, Yuheng Li, Krishna Kumar Singh, Richard Zhang, Eli Shechtman, Jun-Yan Zhu, and Xun Huang. Learning an image editing model without image editing pairs. *arXiv preprint arXiv:2510.14978*, 2025. 3
- [18] Kimin Lee, Hao Liu, Moonkyung Ryu, Olivia Watkins, Yuqing Du, Craig Boutilier, Pieter Abbeel, Mohammad Ghavamzadeh, and Shixiang Shane Gu. Aligning text-to-image models using human feedback. *arXiv preprint arXiv:2302.12192*, 2023. 1, 2
- [19] Shanglin Li, Bohan Zeng, Yutang Feng, Sicheng Gao, Xiuhui Liu, Jiaming Liu, Lin Li, Xu Tang, Yao Hu, Jianzhuang Liu, et al. Zone: Zero-shot instruction-guided local editing. In *Proceedings of the IEEE/CVF Conference on Computer Vision and Pattern Recognition*, pages 6254–6263, 2024. 2
- [20] Xuying Li, Zhuo Li, Yuji Kosuga, and Victor Bian. Optimizing safe and aligned language generation: A multi-objective grpo approach. *arXiv preprint arXiv:2503.21819*, 2025. 1
- [21] Yaowei Li, Yuxuan Bian, Xuan Ju, Zhaoyang Zhang, Junhao Zhuang, Ying Shan, Yuexian Zou, and Qiang Xu. Brushedit: All-in-one image inpainting and editing. *arXiv preprint arXiv:2412.10316*, 2024. 2
- [22] Tsung-Yi Lin, Michael Maire, Serge Belongie, James Hays, Pietro Perona, Deva Ramanan, Piotr Dollár, and C Lawrence Zitnick. Microsoft coco: Common objects in context. In *European conference on computer vision*, pages 740–755. Springer, 2014. 5, 4
- [23] Jie Liu, Gongye Liu, Jiajun Liang, Yangguang Li, Jiaheng Liu, Xintao Wang, Pengfei Wan, Di Zhang, and Wanli Ouyang. Flow-grpo: Training flow matching models via online rl. *arXiv preprint arXiv:2505.05470*, 2025. 1, 3
- [24] Luping Liu, Chao Du, Tianyu Pang, Zehan Wang, Chongxuan Li, and Dong Xu. Improving long-text alignment for text-to-image diffusion models. *arXiv preprint arXiv:2410.11817*, 2024. 3

- [25] Shiyu Liu, Yucheng Han, Peng Xing, Fukun Yin, Rui Wang, Wei Cheng, Jiaqi Liao, Yingming Wang, Honghao Fu, Chunrui Han, et al. Step1x-edit: A practical framework for general image editing. *arXiv preprint arXiv:2504.17761*, 2025. 1, 2, 6
- [26] Zeyu Lu, Chengyue Wu, Xinyuan Chen, Yaohui Wang, Lei Bai, Yu Qiao, and Xihui Liu. Hierarchical diffusion autoencoders and disentangled image manipulation. In *Proceedings of the IEEE/CVF Winter Conference on Applications of Computer Vision*, pages 5374–5383, 2024. 1
- [27] Or Patashnik, Daniel Garibi, Idan Azuri, Hadar Averbuch-Elor, and Daniel Cohen-Or. Localizing object-level shape variations with text-to-image diffusion models. In *Proceedings of the IEEE/CVF international conference on computer vision*, pages 23051–23061, 2023. 2
- [28] William Peebles and Saining Xie. Scalable diffusion models with transformers. In *Proceedings of the IEEE/CVF international conference on computer vision*, pages 4195–4205, 2023. 1
- [29] Zhihong Shao, Peiyi Wang, Qihao Zhu, Runxin Xu, Junxiao Song, Xiao Bi, Haowei Zhang, Mingchuan Zhang, YK Li, Yang Wu, et al. Deepseekmath: Pushing the limits of mathematical reasoning in open language models. *arXiv preprint arXiv:2402.03300*, 2024. 1, 2
- [30] Bram Wallace, Meihua Dang, Rafael Rafailov, Linqi Zhou, Aaron Lou, Senthil Purushwalkam, Stefano Ermon, Caiming Xiong, Shafiq Joty, and Nikhil Naik. Diffusion model alignment using direct preference optimization. In *Proceedings of the IEEE/CVF Conference on Computer Vision and Pattern Recognition*, pages 8228–8238, 2024. 1, 2
- [31] Hongcheng Wang, YINUO Huang, Sukai Wang, Guanghui Ren, and Hao Dong. Grpo-ma: Multi-answer generation in grpo for stable and efficient chain-of-thought training. *arXiv preprint arXiv:2509.24494*, 2025. 1
- [32] Qian Wang, Biao Zhang, Michael Birsak, and Peter Wonka. Instructedit: Improving automatic masks for diffusion-based image editing with user instructions. *arXiv preprint arXiv:2305.18047*, 2023. 2
- [33] Yibin Wang, Zhimin Li, Yuhang Zang, Yujie Zhou, Jiazi Bu, Chunyu Wang, Qinglin Lu, Cheng Jin, and Jiaqi Wang. Pref-grpo: Pairwise preference reward-based grpo for stable text-to-image reinforcement learning. *arXiv preprint arXiv:2508.20751*, 2025. 1, 3
- [34] Zhenyu Wang, Aoxue Li, Zhenguo Li, and Xihui Liu. Genartist: Multimodal llm as an agent for unified image generation and editing. *Advances in Neural Information Processing Systems*, 37:128374–128395, 2024. 2, 1
- [35] Chenfei Wu, Jiahao Li, Jingren Zhou, Junyang Lin, Kaiyuan Gao, Kun Yan, Sheng-ming Yin, Shuai Bai, Xiao Xu, Yilei Chen, et al. Qwen-image technical report. *arXiv preprint arXiv:2508.02324*, 2025. 1, 2, 6
- [36] Chenyuan Wu, Pengfei Zheng, Ruiran Yan, Shitao Xiao, Xin Luo, Yueze Wang, Wanli Li, Xiyan Jiang, Yexin Liu, Junjie Zhou, et al. Omnigen2: Exploration to advanced multimodal generation. *arXiv preprint arXiv:2506.18871*, 2025. 2, 6
- [37] Xiaoshi Wu, Yiming Hao, Manyuan Zhang, Keqiang Sun, ZhaoYang Huang, Guanglu Song, Yu Liu, and Hongsheng Li. Deep reward supervisions for tuning text-to-image diffusion models. In *European Conference on Computer Vision*, pages 108–124. Springer, 2024. 2, 3, 5
- [38] Yongliang Wu, Zonghui Li, Xinting Hu, Xinyu Ye, Xianfang Zeng, Gang Yu, Wenbo Zhu, Bernt Schiele, Ming-Hsuan Yang, and Xu Yang. Kris-bench: Benchmarking next-level intelligent image editing models. *arXiv preprint arXiv:2505.16707*, 2025. 1, 6
- [39] Shitao Xiao, Yueze Wang, Junjie Zhou, Huaying Yuan, Xingrun Xing, Ruiran Yan, Chaofan Li, Shuting Wang, Tiejun Huang, and Zheng Liu. Omnigen: Unified image generation. In *Proceedings of the Computer Vision and Pattern Recognition Conference*, pages 13294–13304, 2025. 1, 2
- [40] Zeyue Xue, Jie Wu, Yu Gao, Fangyuan Kong, Lingting Zhu, Mengzhao Chen, Zhiheng Liu, Wei Liu, Qiushan Guo, Weilin Huang, et al. Dancegrpo: Unleashing grpo on visual generation. *arXiv preprint arXiv:2505.07818*, 2025. 1, 3
- [41] Chun-Hsiao Yeh, Yilin Wang, Nanxuan Zhao, Richard Zhang, Yuheng Li, Yi Ma, and Krishna Kumar Singh. Beyond simple edits: X-planner for complex instruction-based image editing. *arXiv preprint arXiv:2507.05259*, 2025. 2, 1
- [42] Qifan Yu, Wei Chow, Zhongqi Yue, Kaihang Pan, Yang Wu, Xiaoyang Wan, Juncheng Li, Siliang Tang, Hanwang Zhang, and Yueting Zhuang. Anyedit: Mastering unified high-quality image editing for any idea. In *Proceedings of the Computer Vision and Pattern Recognition Conference*, pages 26125–26135, 2025. 1, 2, 6
- [43] Kai Zhang, Lingbo Mo, Wenhua Chen, Huan Sun, and Yu Su. Magicbrush: A manually annotated dataset for instruction-guided image editing. *Advances in Neural Information Processing Systems*, 36:31428–31449, 2023. 1, 2, 6
- [44] Shu Zhang, Xinyi Yang, Yihao Feng, Can Qin, Chia-Chih Chen, Ning Yu, Zeyuan Chen, Huan Wang, Silvio Savarese, Stefano Ermon, et al. Hive: Harnessing human feedback for instructional visual editing. In *Proceedings of the IEEE/CVF Conference on Computer Vision and Pattern Recognition*, pages 9026–9036, 2024. 3
- [45] Tianrui Zhu, Shiyi Zhang, Jiawei Shao, and Yansong Tang. Kv-edit: Training-free image editing for precise background preservation. *arXiv preprint arXiv:2502.17363*, 2025. 2

CogniEdit: Dense Gradient Flow Optimization for Fine-Grained Image Editing

Supplementary Material

6. Algorithm

We provide the training procedure for CogniEdit, which combines Dynamic Token Focus Relocation with Dense GRPO Optimization.

Algorithm 1 Training Procedure of CogniEdit

Require: Policy π_θ , reference π_{ref} , reward model R , MLLM, batch size B , group size G , timesteps T , dense steps k

- 1: Initialize θ , token focus predictor p_η , soft tokens $\{s_i^{1:k}\}_{i=1}^N$
- 2: **for** each training iteration **do**
- 3: Sample batch $\{(\text{image}_b, \text{instruction}_b)\}_{b=1}^B$
- 4: Decompose instructions: $c_b \leftarrow \text{MLLM.decompose}(\text{instruction}_b)$ for $b = 1, \dots, B$
- 5: **Dynamic Token Focus:** For each layer i , predict $\text{pos} \leftarrow p_\eta(h_i^l)$ and inject $h_i^{\text{pos:pos}+k} \leftarrow s_i^{1:k}$
- 6: **for** $b = 1$ to B **do**
- 7: Sample $r \sim \text{Uniform}[k, T]$ and initialize $x_r^{b,1:G}$
- 8: **for** $i = 1$ to G **do**
- 9: Denoise k steps: $x_{t-1}^{b,i} \leftarrow x_t^{b,i} - \frac{1}{T}(v_\theta(\text{sg}(x_t^{b,i}), t) + \frac{\sigma_t^2}{2}[x_t^{b,i} + (1 - t)v_\theta(\text{sg}(x_t^{b,i}), t)]) + \frac{\sigma_t}{\sqrt{T}}\epsilon$ for $t = r, \dots, r - k$
- 10: Complete: $x_0^{b,i} \leftarrow \text{sg}(\text{Denoise}(x_{r-k}^{b,i}))$
- 11: Evaluate: $R(x_0^{b,i}, c_b)$
- 12: **end for**
- 13: **end for**
- 14: Compute the batch advantages: $\hat{A}^b \leftarrow \frac{1}{G} \sum_{i=1}^G \frac{R(x_0^{b,i}, c_b) - \mu_{\text{batch}}}{\sigma_{\text{batch}}}$ where $\mu_{\text{batch}}, \sigma_{\text{batch}}$ are batch statistics
- 15: Compute probability ratios: $\tilde{r}_b^{r:r-k}(\theta) \leftarrow \exp(\text{clip}(\sum_{t=r}^{r-k+1} \log \frac{p_\theta(x_{t-1}^b | x_t^b, c_b)}{p_{\theta_{\text{old}}}(x_{t-1}^b | x_t^b, c_b)}, -\log(1 + \epsilon), \log(1 + \epsilon)))$
- 16: Compute optimization objective: $\mathcal{J}_{\text{Dense}}(\theta) \leftarrow \frac{1}{B} \sum_{b=1}^B \min(\tilde{r}_b^{r:r-k} \hat{A}^b, \text{clip}(\tilde{r}_b^{r:r-k}, 1 - \epsilon, 1 + \epsilon) \hat{A}^b) - \hat{\beta} D_{\text{KL}}(\pi_\theta \| \pi_{\text{ref}})$
- 17: Update: $\theta, \eta, \{s_i^{1:k}\}_{i=1}^N \leftarrow$ gradient step on maximizing $\mathcal{J}_{\text{Dense}}(\theta)$
- 18: **end for**
- 19: **return** $\pi_\theta, p_\eta, \{s_i^{1:k}\}_{i=1}^N$

The algorithm integrates three key components: (1) MLLM-based instruction decomposition for semantic understanding, (2) Dynamic Token Focus Relocation for hierarchical attention patterns, and (3) Dense GRPO Optimization with gradient accumulation across k consecutive de-

noising steps. The batch-level advantage computation stabilizes training for editing tasks, while stop gradient operations ensure proper gradient flow through the sampling trajectory.

7. Background

7.1. Stop Gradient

Stop gradient is a technique that selectively blocks gradient flow through specific computational paths during backpropagation. In neural network training, gradients typically flow backward through all operations to update model parameters. However, in certain scenarios, allowing unrestricted gradient flow can lead to training instability or undesired parameter updates. By applying stop gradient operations, denoted as $\text{sg}(\cdot)$, we can treat certain values as constants during the backward pass while preserving their computational graph during the forward pass.

Formally, for a tensor x , the stop gradient operation is defined as:

$$y = \text{sg}(f(x)), \quad \text{where} \quad \frac{\partial y}{\partial x} = 0 \quad (10)$$

During forward propagation, $y = f(x)$, but during backpropagation, no gradients flow through this operation. This is particularly useful in reinforcement learning and self-supervised learning scenarios where we want to compute values based on the current model state without updating certain components.

In our framework, we strategically employ stop gradient operations to stabilize training when computing target values or baseline estimates that should not directly influence certain model components through gradient descent, as we detail in Section 3.3.

8. Methodology

8.1. Visual Reasoning Enhanced Text Encoding

Visual reasoning enhanced text encoding leverages vision-language models (VLMs) to generate enriched text representations that exhibit superior alignment with visual content. Recent research has demonstrated that exploiting the reasoning capabilities of VLMs to extract detailed, fine-grained visual information yields more effective guidance for model behavior [34, 41]. This approach addresses the limitation of naive text encoding, which often fails to capture the nuanced semantic relationships between instructions and visual content necessary for precise editing operations.

Input

Ours

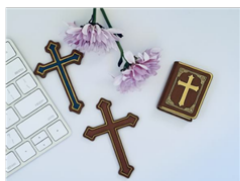
Qwen-Image

OmniGen2

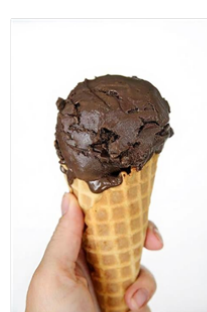
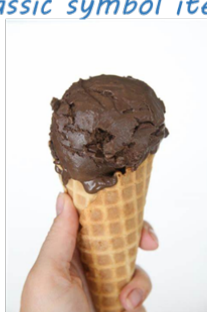
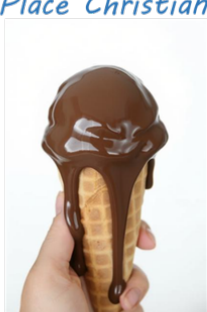
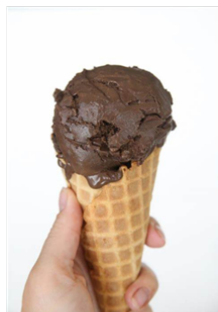
Step1X-Edit



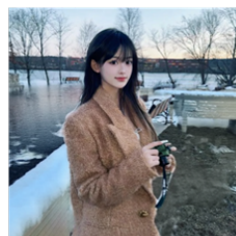
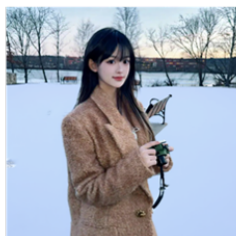
"Correct the Incorrect Driving Habits in the Image"



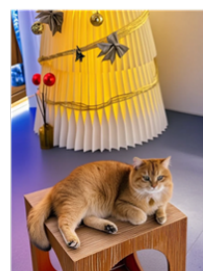
"Place Christian classic symbol items on the table"



"Change to resemble the appearance after being exposed under the sun for half an hour"



"Add some snow to the background"



"Apply a suitable filter for this image"



"Make the ice cream jade"

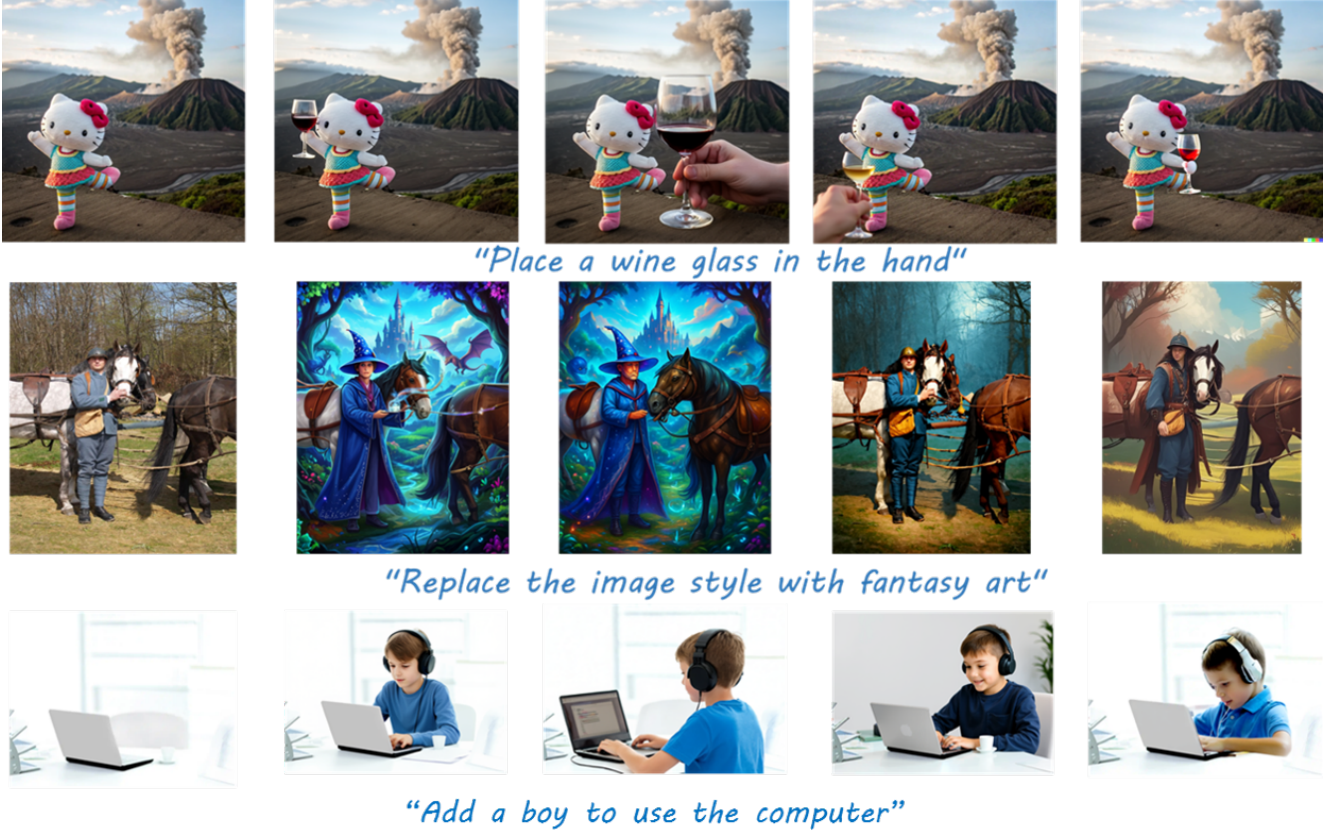


Figure 9. Qualitative comparison with instruction-based editing methods. CogniEdit maintains high visual quality and natural blending between edited and unedited regions, while baseline methods struggle with consistency preservation.

The encoding process follows a structured reasoning pipeline. Given an editing instruction and source image, the VLM performs hierarchical semantic analysis through three stages: (1) **Visual Comprehension** – generating a detailed image description encompassing objects, quantities, textual elements, spatial relationships, and salient visual features; (2) **Reasoning** – constructing a logical reasoning chain that connects the visual content with the editing instruction; (3) **Instruction Synthesis** – producing an enriched editing instruction that incorporates both the original command and contextual visual information.

To further enhance editing precision, we extend this standard reasoning framework with an additional **Target Specification** stage that explicitly identifies and describes the specific image regions or objects to be modified. This four-stage reasoning process provides comprehensive semantic grounding for the editing model, enabling more accurate interpretation of editing intents.

Formally, we prompt the VLM to generate structured outputs following the format:

- **Caption** (`<info>`): A comprehensive visual description capturing objects, quantities, text, spatial relations, and

salient features;

- **Reasoning** (`<think>`): A logical reasoning chain connecting visual content with the editing instruction;
- **Answer** (`<answer>`): An enriched editing instruction synthesizing original command and visual context;
- **Target** (`<object>`): Detailed specification of regions or objects to be modified.

The complete output structure is thus:

```

<info>...</info> <think>...</think>
<answer>...</answer> <object>...</object>
(11)

```

,which provides the editing model with multi-level semantic guidance ranging from holistic scene understanding to precise target localization.

8.2. Data Preparation

We construct our training dataset by combining existing editing datasets with self-constructed data, resulting in a diverse collection of image editing pairs. Specifically, we utilize the following data sources:



Figure 10. Qualitative comparison with knowledge-based editing methods. Each example shows source image, instruction requiring domain knowledge or reasoning, and results from different methods.

- **SEED-Data-Edit** [11]³: We sample 3k editing pairs from Part 2 of this dataset, which comprises real-world editing scenarios collected from the internet.

³<https://huggingface.co/datasets/AILab-CVC/SEED-Data-Edit>

- **COCO 2017** [22]⁴: We randomly select 1k images from the COCO 2017 dataset and construct corresponding editing pairs.

⁴<https://cocodataset.org/>

For the self-constructed COCO-based data, we employ a systematic approach to generate editing pairs. For each selected image, we apply instance segmentation to obtain object masks and select the largest segment as the target editing region based on mask area. We then create editing instructions following the template: “Add a green segmentation mask (for object detection) to the *[object name]* on the *[position]* of the image”, where *[object name]* and *[position]* are automatically determined from the segmentation results. This construction process yields paired data consisting of the original image, the edited image with the applied mask, and the corresponding text instruction.

9. Knowledge-enhanced instruction

Complex editing instructions often contain implicit semantic requirements or require domain knowledge that is challenging for editing models to directly interpret. For instance, an instruction like “Replace the sky with a sunset scene” requires understanding what constitutes a visually plausible sunset (warm color gradients, sun position, atmospheric effects), while “Change the car to a sports car” demands knowledge of typical sports car characteristics (low profile, aerodynamic design, distinctive features). To bridge this semantic gap, we leverage Multi-modal Large Language Models (MLLMs) to decompose and enhance editing instructions with explicit, actionable guidance.

MLLM-based Instruction Enhancement. Given a source image and an editing instruction, we employ an MLLM (specifically, PeBR-R1-7b [7]) to analyze the visual content and generate a knowledge-enhanced instruction. The enhancement process follows a structured prompt template that guides the MLLM to:

- **Semantic Decomposition:** Break down abstract editing requests into specific visual attributes (colors, shapes, positions, textures).
- **Knowledge Injection:** Incorporate domain-specific knowledge relevant to the editing task (e.g., anatomical correctness, physical plausibility).
- **Spatial Grounding:** Provide explicit spatial references to guide precise localization of editing regions.

The used template is presented in Figure 12. The MLLM processes both the image and instruction, generating enhanced instructions that explicitly specify editing details. And we provide samples of the enhanced instructions in Figure 13, including the description of the input image, the think process and the enhanced instruction. The knowledge enhancement provides several key advantages. First, it transforms ambiguous instructions into explicit specifications, reducing the model’s burden of implicit reasoning during the editing process. Second, it ensures semantic consistency by incorporating factual knowledge (e.g., correct number of petals for specific flowers, appropriate proportions for objects). Third, it provides fine-grained attribute

specifications that align with our Dynamic Token Focus Relocation mechanism—the enhanced instructions contain more tokens describing precise attributes, which our mechanism can effectively emphasize during processing.

10. Experiment

10.1. Reward Model

Effective reward signals are critical for GRPO optimization. We design a comprehensive reward model based on Multi-modal Large Language Models (MLLMs) that evaluates edited images across multiple dimensions. Unlike single-metric rewards (e.g., CLIP score) that only measure text-image alignment, our reward model provides multi-faceted evaluation considering instruction following, visual coherence, and source consistency—essential criteria for high-quality image editing.

MLLM-based Reward Evaluation. We employ Qwen2.5-VL-7B-Instruct as our reward model. Given an edited image, the original image, and the editing instruction, the model evaluates the editing quality through a structured prompt that assesses multiple aspects:

1. **Word-level Analysis:** Extract key words related to subjects, objects, colors, numbers, lighting, style, and activities in the instruction, scoring how well each element is visually represented in the edited image. A special token `[No_mistakes]` indicates whether all elements are correctly depicted.
2. **Holistic Assessment:** Provide overall scores on four axes (each rated 1-5):
 - *Alignment Score:* How well the edited image matches the instruction in terms of content.
 - *Coherence Score:* Logical consistency of the image, including absence of visual glitches, object distortions, location errors, or incorrect colors/quantities.
 - *Style Score:* Aesthetic quality and visual appeal of the edited image.
 - *Consistency Score:* Fidelity to the original image in unedited regions.

The complete reward prompt is:

You are presented with an edited image (the first image) and its original image (the second image), and the associated text caption of the edited image. Your task is to analyze the edited image across multiple dimensions in relation to the caption and its original image. Specifically:

1. Extract key words related to: subject, object, color, number, lighting, style and activities in the caption based on how well it is visually represented in the edited image. - A higher score indicates that the word is less well represented in the image. - The special token [No_mistakes] represents whether all elements in the caption were correctly depicted. A high score suggests no mistakes; a low score suggests missing or incorrect

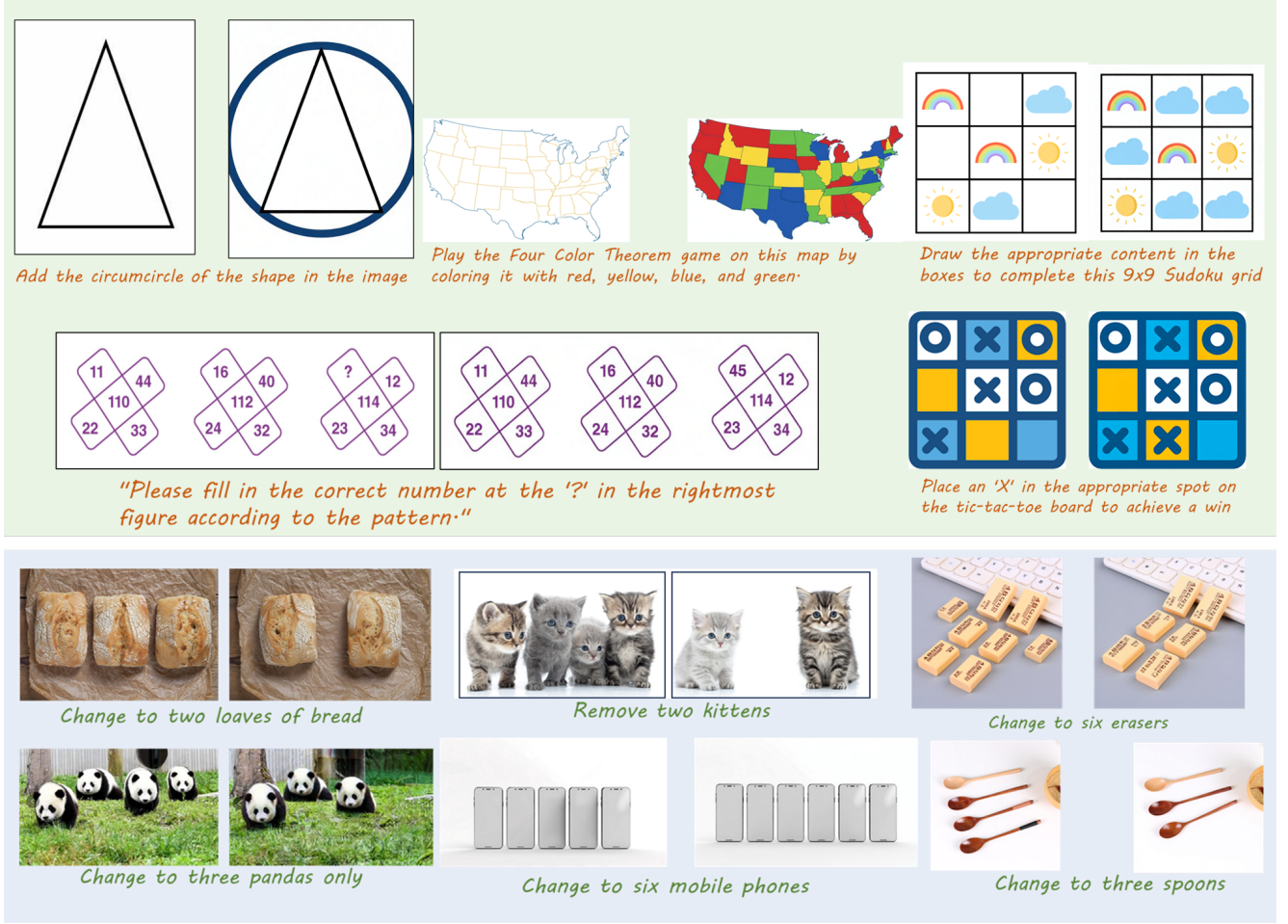


Figure 11. The editing results of our method on Kris-Bench.

elements. 2. Provide overall assessments for the image along the following axes (each rated from 1 to 5):

- Alignment Score: How well the image matches the caption in terms of content.
- Coherence Score: How logically consistent the image is (object location error, absence of visual glitches, object distortions, object is missing or extra, color or quantity error etc.).
- Style Score: How aesthetically appealing the image looks, regardless of caption accuracy.
- Consistency Score: How well the edited image consistent to its original image.

Output your evaluation using the format below and also provide the reason why you give this score: Alignment Score (1-5): X Coherence Score (1-5): Y Style Score (1-5): Z Consistency Score (1-5): W Output the basis and reasons for the scores given above.

Reward Computation. From the MLLM’s structured output, we extract three key metrics to compute the final reward. We exclude the Style Score as it measures aesthetic appeal independent of editing correctness. The reward R

for each edited image is computed as:

$$R = S_{\text{alignment}} + S_{\text{coherence}} + S_{\text{consistency}}, \quad (12)$$

where $S_{\text{alignment}}$, $S_{\text{coherence}}$, and $S_{\text{consistency}}$ are the alignment, coherence, and consistency scores respectively, each normalized to [0, 5]. This formulation balances three critical aspects: (1) instruction-image alignment ensures the edit follows the textual specification, (2) coherence prevents visual artifacts and semantic inconsistencies, and (3) consistency preserves the integrity of unedited regions. By averaging these three scores, we obtain a holistic reward that guides the model to produce edits that are simultaneously accurate, plausible, and faithful to the source image. We provide the samples of how the reward model evaluates the edited image in Figure 14.

Advantages of MLLM-based Rewards. Compared to traditional metrics like CLIP score or learned discriminators, our MLLM-based reward model offers several advantages. First, it provides interpretable, fine-grained feedback through word-level analysis and multi-dimensional scoring.

Prompt: You are tasked with analyzing an image to generate an exhaustive and detailed description. Your goal is to extract and describe all possible information from the image, including but not limited to objects, numbers, text, and the relationships between these elements. The description should be as fine and detailed as possible, capturing every nuance. After generating the detailed description, you need to analyze the instruction and provide step-by-step simple reasoning for the given instruction, please avoid repeating the same points. Finally, provide concise answer to what will happen with the given instruction and provide the specific instruction to modify the image, and list the properties of the modified image, including number, color and position of the object. The description, reasoning process, answer and property are enclosed within <info> </info>, <think> </think>, <answer> </answer> and <object> </object> tags, respectively, i.e., <info> image description here </info> <think> reasoning process here </think> <answer> answer here </answer> <object> list the perperties of modified image here </object>.

Figure 12. The template used for instruction enhancement.

Second, it can evaluate complex semantic correctness (e.g., correct number of objects, appropriate spatial relationships) beyond simple feature matching. Third, by conditioning on both the source and edited images, it explicitly evaluates source consistency—a crucial aspect often overlooked by generation-focused metrics. Empirically, we find that this reward formulation leads to more stable training and better alignment with human preferences compared to single-metric alternatives.

10.2. Results on GEdit-Bench

Editability Preservation. Our dense reward optimization is specifically designed to enhance fine-grained alignment with detailed prompt features (e.g., precise colors, positions, quantities), which represents a different optimization objective than general-purpose editing. To assess whether this specialization compromises broader editing capabilities, we evaluate on GEdit-Bench with three metrics: Q_SC (source consistency), Q_PQ (edited quality), and Q_O (overall quality), evaluated by QwenVL-2.5-72B. As shown in Table 3, our method maintains competitive performance across both the intersection subset and full set, with scores comparable to top-performing general-purpose models like Qwen-Image and Step1X-Edit. While slight variations in individual metrics reflect the inherent trade-off between optimizing for fine-grained precision versus general editing flexibility, our method does not exhibit significant degradation despite being optimized for a more specialized objective. These results validate our design choice: we achieve

substantial improvements on fine-grained tasks (as shown in Kris-Bench) without sacrificing competitiveness on general editing scenarios, demonstrating that dense reward optimization successfully balances fine-grained instruction following with general editability. The editing results of our

Table 3. The results on the GEdit-Bench, where Q_SC is the quality score of the source image, Q_PQ is the quality score of the edited image, and Q_O is the quality score of the edited image..

Method	Intersection subset			Full set		
	Q_SC	Q_PQ	Q_O	Q_SC	Q_PQ	Q_O
InsPix2Pix	4.833	6.992	4.691	4.746	6.913	4.578
MagicBrush	5.814	7.149	5.653	5.752	7.069	5.558
AnyEdit	3.873	6.754	3.789	3.713	6.730	3.635
Step1X-Edit	7.501	7.264	7.189	7.388	7.279	7.067
OmniGen2	6.584	7.233	6.295	6.618	7.191	6.296
Qwen-Image-Edit	7.819	7.398	7.462	7.752	7.394	7.402
Ours	<u>7.723</u>	7.441	<u>7.408</u>	<u>7.618</u>	7.417	<u>7.285</u>

method on the GEdit-Bench are shown in Figure 15.

10.3. Visualization

We provide qualitative comparisons to demonstrate CogniEdit’s superiority in handling fine-grained instructions and knowledge-intensive editing tasks. The visualizations illustrate how our method achieves superior instruction following while maintaining visual quality and source consistency.

Compare to Instruction-based methods. Figure 9 presents qualitative comparisons between CogniEdit and state-of-the-art instruction-based editing methods: Qwen-Image-Edit-r1, Step1X-Edit, and OmniGen2. These examples highlight scenarios requiring precise attribute control, including exact color specifications, numerical quantities, and spatial positioning.

The visual comparisons reveal critical differences in fine-grained instruction following capabilities. CogniEdit consistently captures precise specifications that baseline methods fail to reproduce. Step1X-Edit and OmniGen2 exhibit particular difficulty with numerical attributes and spatial positioning, often ignoring these fine-grained details in favor of general semantic understanding. Qwen-Image-Edit-r1 performs better but still shows inconsistent handling of multi-attribute instructions. These results validate that our Dense GRPO Optimization and Dynamic Token Focus Relocation mechanism effectively enhance fine-grained attribute control.

Comparison with Knowledge-based Methods. Figure 10 compares CogniEdit against closed-source commercial VLM systems (Gemini 2, Doubao, GPT-4O) and chain-of-thought reasoning methods (Uni-CoT, UniWorld). These examples focus on knowledge-intensive editing tasks requiring domain expertise, factual knowledge, or complex

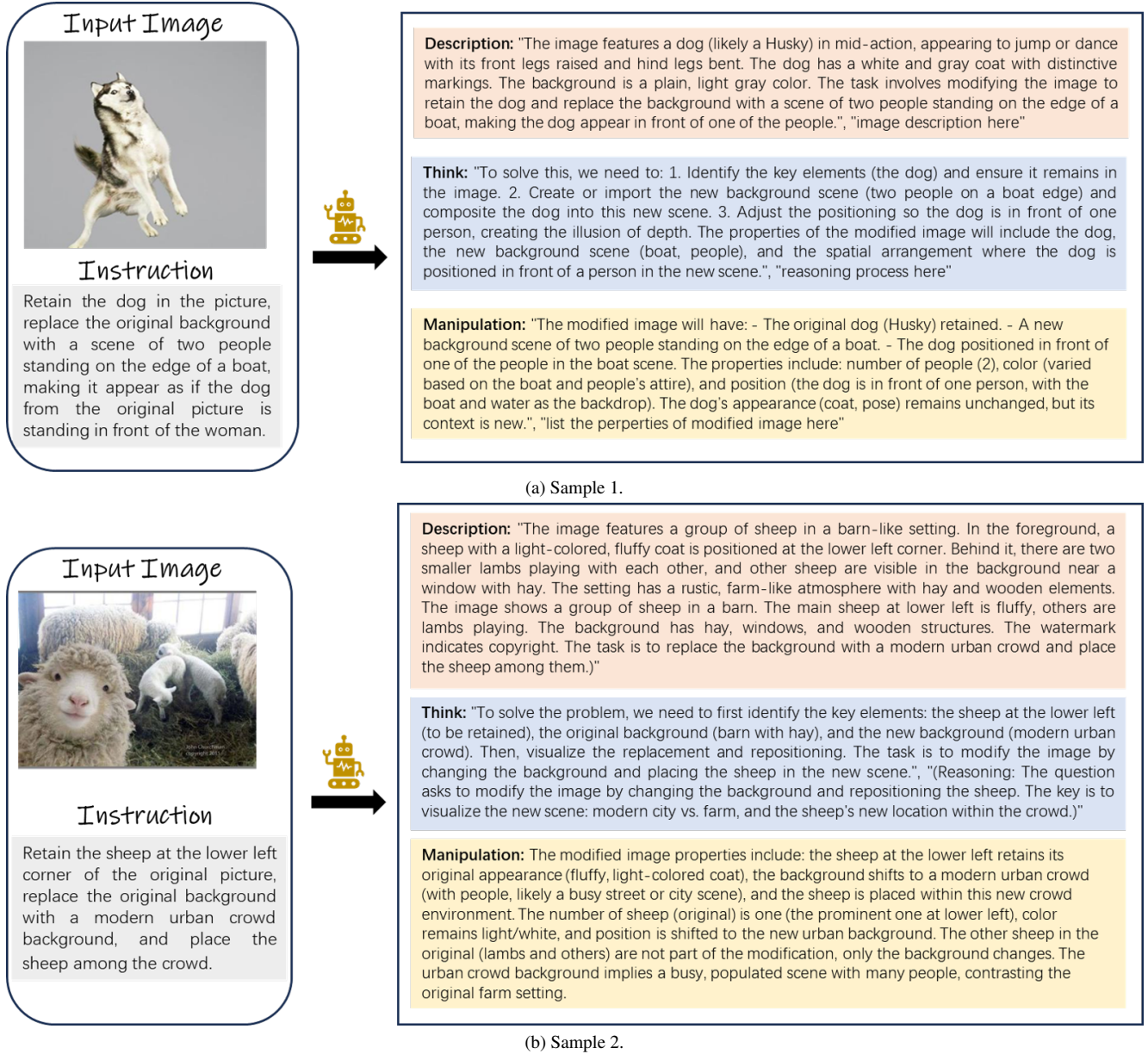


Figure 13. Samples of MLLM-enhanced instruction.

reasoning about visual semantics. We further provide the editing results of our method on Kris-Bench in Figure 11.

The knowledge-based comparisons highlight the importance of balancing semantic correctness with source fidelity. Commercial VLM systems like GPT-4O and Gemini 2 demonstrate strong instruction understanding and can generate semantically plausible content, but they often treat editing as a generation task, leading to poor source consistency—edited images may exhibit different lighting, style, or unnecessary modifications to unedited regions. Doubao shows similar issues with additional artifacts in complex

scenes. Chain-of-thought methods (Uni-CoT, UniWorld) improve reasoning capabilities through explicit decomposition, but their editing quality remains inconsistent, particularly for instructions requiring both reasoning and precise visual control. In contrast, CogniEdit achieves superior balance: the MLLM-based reasoning component ensures semantic correctness and factual knowledge integration, while Dense GRPO Optimization maintains source consistency and visual quality.

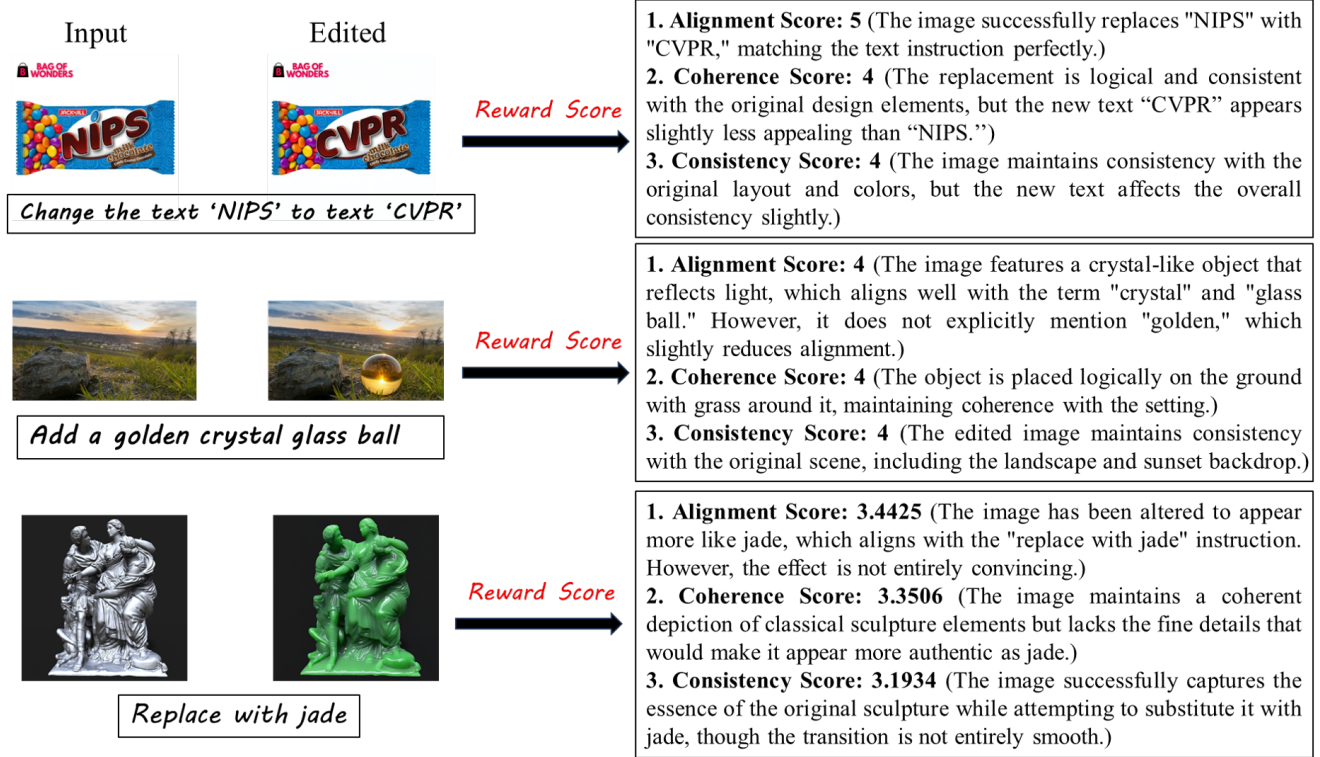


Figure 14. The samples of how the reward model evaluates the edited image.



Figure 15. The editing results of our method on the GEdit-Bench.

10.4. User Study

To assess perceptual quality and editing fidelity from a human perspective, we conduct a comprehensive user study comparing CogniEdit against state-of-the-art instruction-based editing methods and commercial VLM systems. We

recruit 10 participants with diverse backgrounds in computer vision and image editing. Each participant evaluates a series sampled editing pairs from Kris-Bench, ensuring broad coverage of knowledge-intensive scenarios.

Evaluation Protocol. Participants rate each edited image on four criteria using a 5-point Likert scale (1=poor, 5=ex-

cellent):

- **Editing Quality:** Visual plausibility, realism, and absence of artifacts in edited regions.
- **Instruction Adherence:** Alignment between the edited result and the textual instruction, including fine-grained attributes.
- **Consistency:** Preservation of unedited regions and coherence between edited and original content.
- **Overall Score:** Holistic assessment considering all aspects.

The evaluation is double-blind—participants are unaware of which method generated each result, and samples are presented in random order. For each editing task, we compute the mean score across all participants, and overall performance is obtained by averaging across all editing tasks.

For instruction-based editing methods. Table 4 compares CogniEdit against specialized instruction-based editing methods. Our approach achieves the highest scores across all criteria: editing quality (3.71), instruction adherence (3.49), consistency (3.60), and overall performance (3.47). Notably, CogniEdit outperforms the strong baseline Qwen-Image-Edit-r1 by significant margins—7.1% in editing quality and 28.4% in instruction adherence—demonstrating the effectiveness of dense GRPO optimization for fine-grained control.

Table 4. The results of the user study for instruction-based editing methods.

Method	Editing Quality			
	Quality	Adherence	Consistency	Overall
StepIX-Edit	2.743	3.103	2.713	2.790
OmniGen2	2.903	1.984	3.040	2.606
Qwen-Image-Edit-r1	3.468	2.718	3.281	2.968
Ours	3.712	3.487	3.603	3.465

For knowledge-based editing methods. Table 5 compares CogniEdit against commercial VLM systems on knowledge-intensive editing tasks.

Table 5. The results of the user study for knowledge-based editing methods.

Method	Editing Quality			
	Quality	Adherence	Consistency	Overall
Gemini 2	3.021	3.387	2.868	3.215
GPT-4o	3.184	3.450	3.059	3.503
Ours	3.712	3.487	3.603	3.465

CogniEdit significantly outperforms both GPT-4O and Gemini 2 in editing quality (3.71 vs. 3.18 and 3.02) and consistency (3.60 vs. 3.06 and 2.87). Interestingly, GPT-4o achieves the highest instruction adherence (3.45), slightly above our method, but suffers from poor consistency, re-

vealing a fundamental trade-off in VLM-based editing: these systems excel at understanding instructions but struggle to maintain source image fidelity during edits, as they treat editing more like generation tasks. Gemini 2’s particularly weak consistency suggests even stronger generation bias. In contrast, CogniEdit achieves balanced performance across all metrics, validating that MLLM-based reasoning combined with dense reward optimization successfully preserves source consistency while following complex instructions. The overall scores (3.47 for CogniEdit vs. 3.50 for GPT-4o) are competitive, but our superior editing quality and consistency make CogniEdit more suitable for practical editing applications where source preservation is critical.